Supplementary Information

Clemens Simbrunner,[*,†] Francesco Quochi,[‡] Gerardo Hernandez-Sosa,[†] Martin Oehzelt,[¶] Roland Resel,[§] Günter Hesser,[‖] Martin Arndt,[‖] Michele Saba,[‡] Andrea Mura,[‡] Giovanni Bongiovanni,[‡] and Helmut Sitter[†]

Institute of Semiconductor and Solid State Physics, Johannes Kepler University Linz, Austria , Dipartimento di Fisica, Università di Cagliari, SLACS-INFM/CNR, I-09042 Monserrato (CA), Italy , Institute of Experimental Physics, Johannes Kepler University Linz, Austria , Institute of Solid State Physics, Graz University of Technology, Austria , and ZONA (Zentrum f. Oberflächen- und Nanoanalytik), Johannes Kepler University Linz, Austria

E-mail: clemens.simbrunner@jku.at

Phone: +43 (0)732 2468 9658. Fax: +43 (0)732 2468 9696

Growth procedure

All samples have been fabricated on muscovite mica (001) substrates by using hot wall epitaxy (HWE).[1,2] Immediately after cleaving, the mica substrates were transfered via a load lock to the growth chamber providing two seperated HWE reactors equipped with p-6P (TCI) and 6T (Sigma-Aldrich) source material. The system is operated under high vacuum (HV) conditions with a nominal pressure of $9 \cdot 10^{-6}$ mbar. The optimized evaporation temperature for p-6P (6T) is given

[*]To whom correspondence should be addressed
[†]Johannes Kepler University Linz
[‡]Universita di Cagliari
[¶]Johannes Kepler University Linz
[§]Graz University of Technology
[‖]Johannes Kepler University Linz

at 240°C (190°C) leading to a nominal growth rate of 3 nm/min (4.5 nm/min). In order to avoid temperature gradients during growth and to reduce adsorpted species on the surface, the substrate has been pre-heated at 120°C for 30 minutes. The chosen temperature is kept constant during the whole growth procedure. After depositing p-6P for 40 minutes (≅120 nm fiber height) the sample is automatically transfered in HV conditions to the 6T source oven. Subsequently 6T has been deposited.

Optics

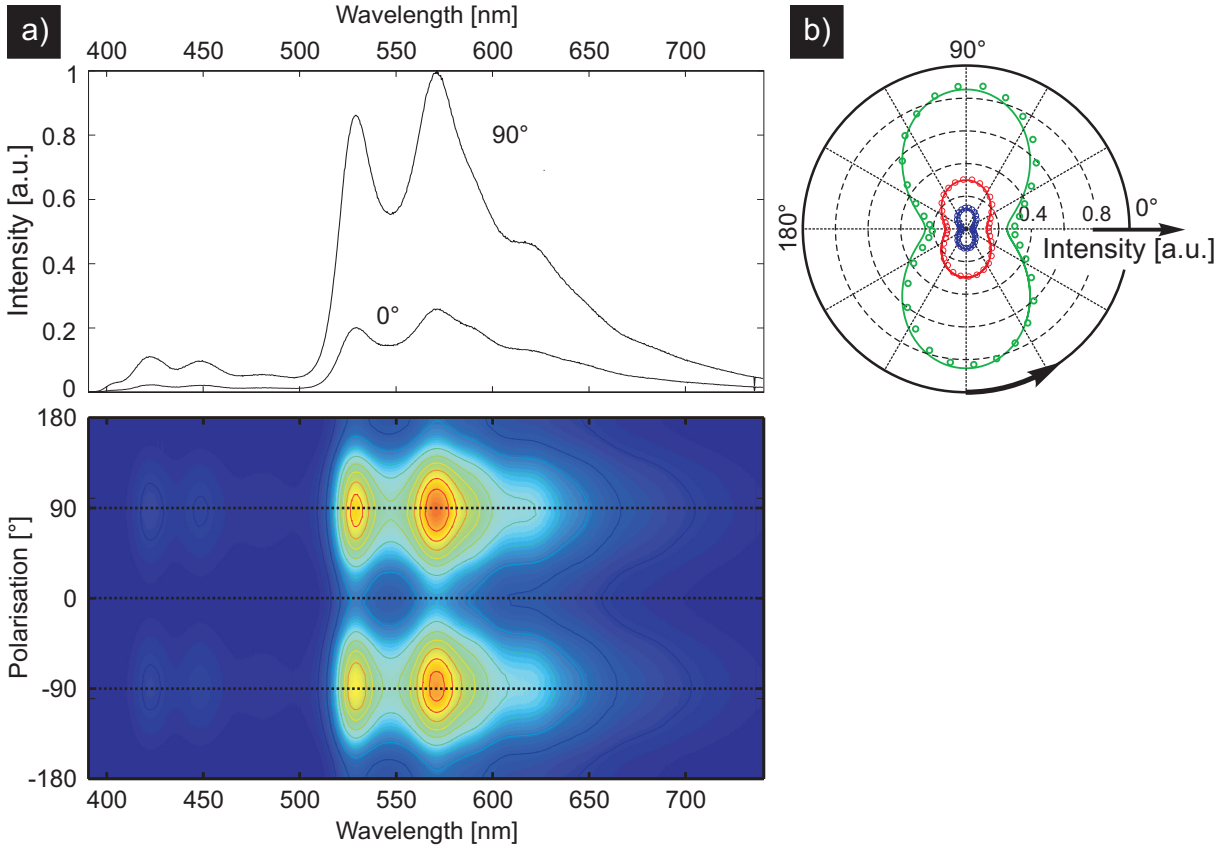

Figure 1: a) Upper panel: Fluorescence spectra of a film with nominally 400 nm 6T fiber thickness, acquired at 0° (long fiber axis) and 90° polarization angle of the excitation (375 nm). The blue, green and red dashed lines represent the fitted contribution of blue (p-6P), green (interfacial 6T submonolayer) and red (crystalline 6T) components. Lower panel: false-colour coded polarization-wavelength spectrogram of the fluorescence intensity. Iso-intensity lines are also displayed. b) Polar plot of the p-6P and 6T material phases fluorescence intensity versus polarization angle of the exciation (Solid lines represent a $\cos^2$ fit to the experimental data).

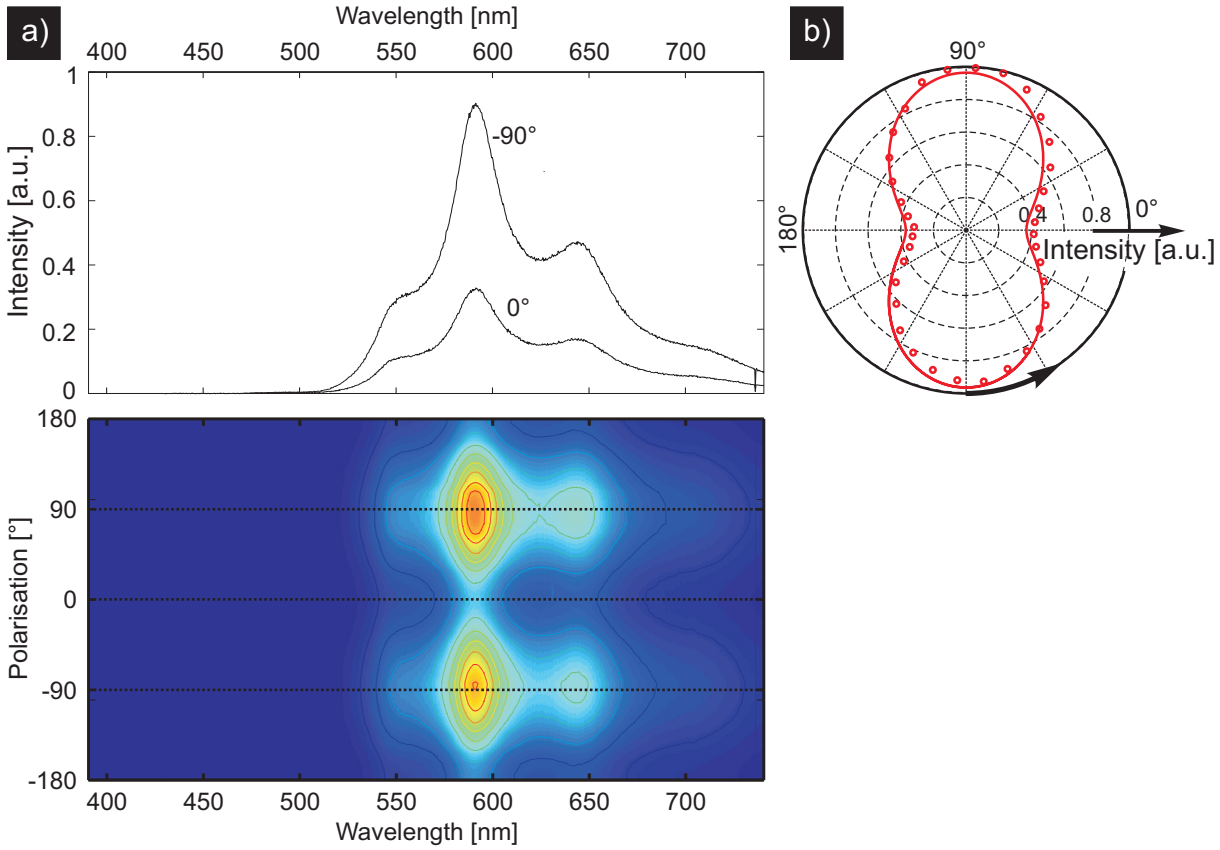

Figure 2: a) Upper panel: Fluorescence spectra of a film with nominally 400 nm 6T fiber thickness, acquired at 0° (long fiber axis) and 90° polarization angle of the excitation (425 nm). The red dashed lines represent the fitted contribution of crystalline 6T components. Lower panel: false-colour coded polarization-wavelength spectrogram of the fluorescence intensity. Iso-intensity lines are also displayed. b) Polar plot of the 6T material phase fluorescence intensity versus polarization angle of the exciation (Solid lines represent a $\cos^2$ fit to the experimental data).

Fluorescence excitation spectroscopy is performed with varying polarization angle of the excitation laser, at 375 nm (see Figure 1) and 425 nm (see Figure 2) pump wavelength. The optical emission spectrum is decomposed in blue, green and red components, which are attributed to crystalline p-6P, interface 6T submonolayer and crystalline 6T, respectively, using the procedure explained in the manuscript. At 375 nm pump wavelentgh, p-6P is directly photoexcited, and optical emission is observed from the three material phases, whereas for 425 nm wavelength pump only 6T crystal emission is observed. We suggest that at 425 nm the optical absorbance of a 6T submonolayer is too small to produce a detectable green fluorescence signal. The polar plots of the spectrally-integrated intensity of p-6P emission with 375 nm pump wavelength and 6T emission

excited at 425 nm (in which case 6T crystals are directly photosensitized), show that the p-6P and 6T crystals possess parallel optical absorption dipoles.

X-ray diffraction

Specular x-ray diffraction as well as x-ray diffraction pole figure measurements were performed in Schultz reflective geometry[3] using CrKα (λ=2.29Å) radiation. The used combination of the collimator size on the primary side and width of the slit optics at the secondary side together with the graphite monochromator results in an acceptance angle of $\pm 0.5^\circ$ around the fixed scattering angle 2Θ of the detector. Based on the observed Bragg peaks of the specular scan as well as on the direction of the poles (net plane normals) within the pole figures, the involved crystallographic phases of the single crystalline muscovite substrate as well as of the organic p-6P, 6T layers could be identified. The used muscovite substrates were $2M_1$-muscovite with monoclinic crystal structure and lattice constants of a=5.20Å, b=9.03Å, c=20.11Å and β=95.782°.[4] The β-structure of sexiphenyl could be identified which represents the equilibrium bulk structure (a=8.091Å, b=5.568Å, c=26.241Å and β=98.17°).[5] In the case of 6T the so called low-temperature polymorph of α-6T could be identified (a =44.708Å, b=7.851Å, c=6.029Å and β = 90.76°.[6]

Table 1: Calculated peak positions used for XRD crystallographic analysis

Crystal	Reflex	Position [Å^{-1}]
Muscovite Mica	(004)	1.2564
p-6P	(11$\bar{1}$)	1.376
6T	($\bar{4}$11)	1.4238

Atomic force microscopy

Atomic force microscopy (AFM) studies of the deposited nano-fibers were performed using a Digital Instruments Dimension 3100 in the tapping mode. The AFM characterization was performed on an area of 10 μm^2 with a SiC tip. The pixel resolution was chosen with 512$\times$512 pixels which

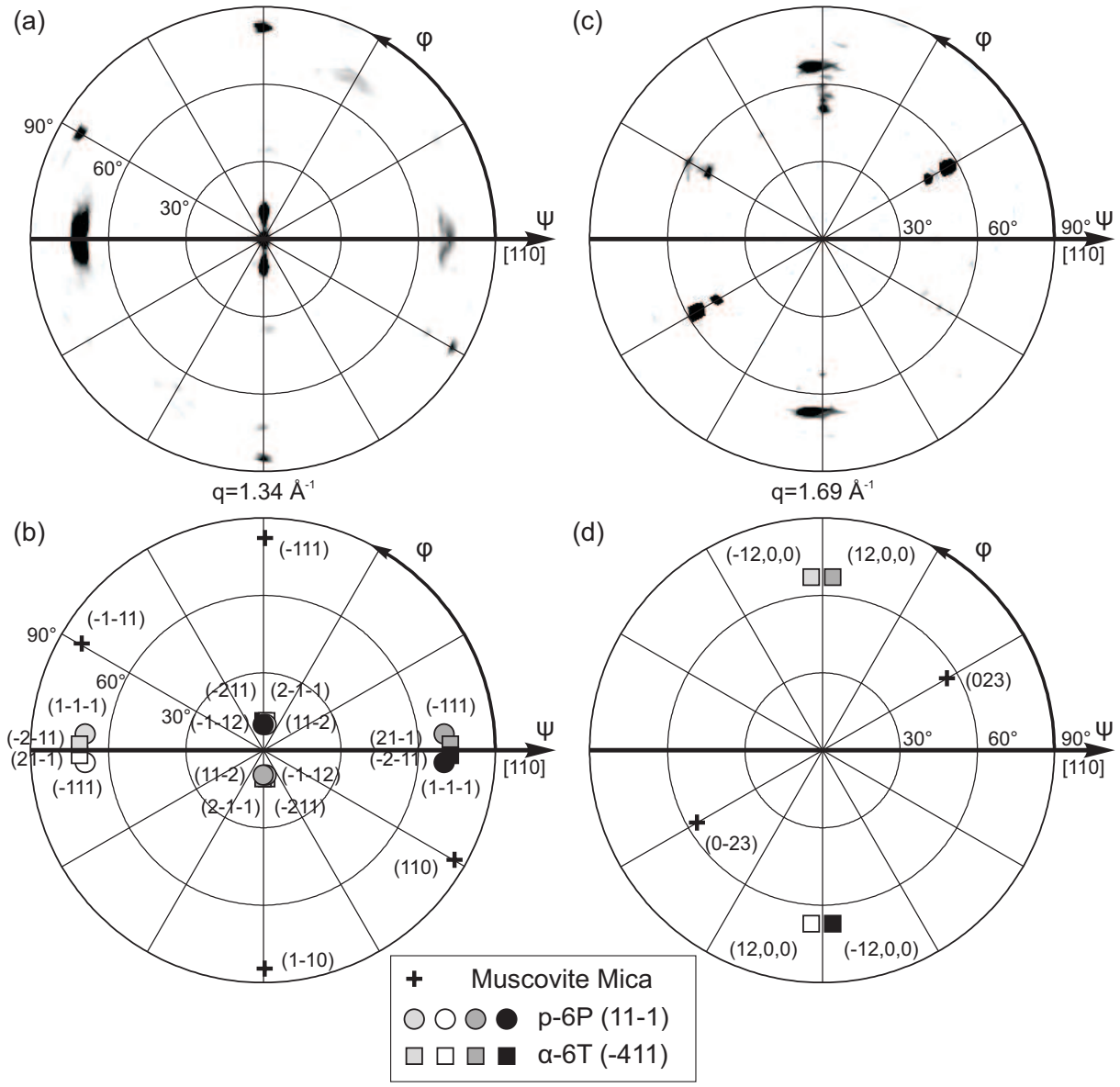

Figure 3: Pole figure measurements of a) (600) p-6P, b) (00.12) 6T reflexes. Plots depicted below (c-d) provide the corresponding stereogram with the simulated positions of the mica (cross) and organic peaks (circles p-6P, rectangles 6T).

corresponds to 19.5 nm/pixel. The zero height has been corrected by leveling the data to the minimum height of the whole image. Images have created by triangulation using a MATLAB routine followed by redering the resulting surface mesh using POVRAY 3.6.

Height histogram data has been deduced from the full area image providing $512 \times 512 = 2^{18}$ datapoints. The height resolution for histogram analysis has been chosen to 2.36 nm. The resulting spectra have been fitted using three different peaks by assuming a Gauss distribution. Resulting fitting parameters are listed in Table 2.

Table 2: Resulting parameters for AFM Height histogram

PeakNr	Parameter	Value	σ^2
1	h_0	10.5 nm	$5.0491 \cdot 10^7$
	I	6911.7	
	$FWHM$	19 nm	
2	h_0	122.6 nm	
	I	2265.3	
	$FWHM$	84 nm	
3	h_0	465.5 nm	
	I	861.0	
	$FWHM$	210 nm	

TEM

In order to provide a proper slide for TEM analysis the sample has been covered by a nominally 50 nm thick aluminium layer for protection purposes. Transmission electron microscopy (TEM) measurements were carried out on a JEOL 2011 microscope (200 kV, LaB6) attached with an OXFORD EDX-System for elemental analysis. Sample preparation with the focused ion beam technique was carried out using a ZEISS XB 1540 Crossbeam after depositing an aluminium protection layer by thermal evaporation. An overview along a typical cross-section is indicated in Figure 4.

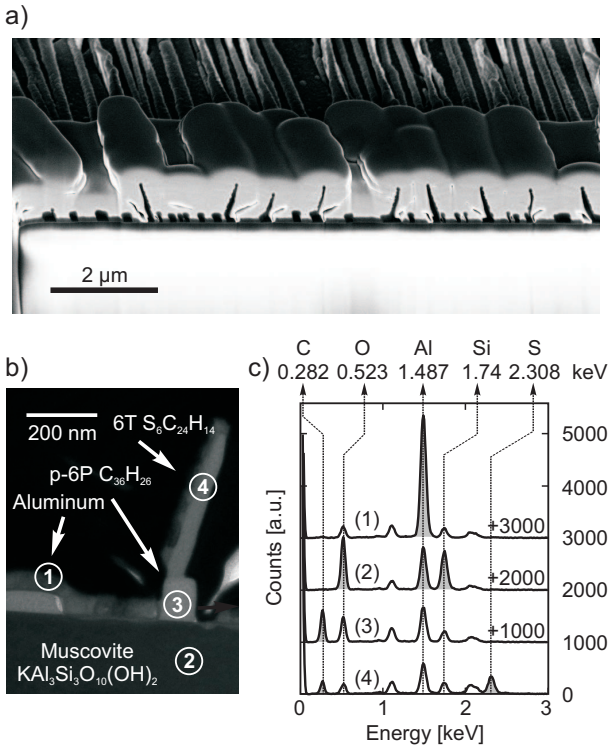

Figure 4: a) Cross-sectional view of the prepared sample provided by SEM. The bright area in the bottom part of the image indicates the mica substrate whereas gray colored regions on top indicate the in-situ deposited protection layer. Dark regions indicate organic nano-fibers. b) TEM image of one single nano-fiber. Numbers indicate regions where EDX spectra have been taken. c) EDX spectra originating from 1) aluminium protection layer 2) muscovite mica substrate 3) p-6P 4) 6T

Scanning Auger

After TEM measurements the sample has been transfered to a scanning Auger microscope. The Auger images were taken at a tilt angle of 30° to the 30 kV primary electron beam and 30° to the concentric hemispherical analyzer (CHA) as a good compromise between distorsion and count rate. The primary electron beam current was set to 10 nA and the CHA operated in constant analyser energy (CAE) mode with a pass energy of 500 eV to obtain maximum count rate at the expense of energy resolution of 10eV. Each Auger image consists of 128x128 pixels with a dwell time 50 ms per pixel. For the Al and the C image the KLL Auger peaks at 1389 eV and 263 eV were used and for the S mapping the LVV Auger peak at 146 eV, respectively.

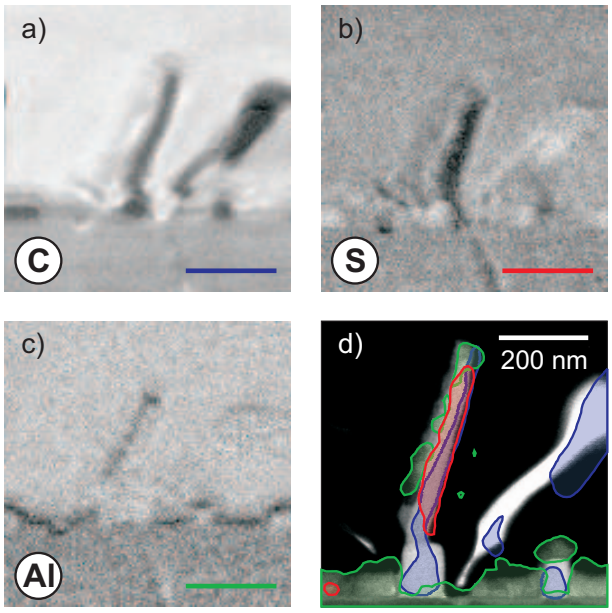

Figure 5: a)-c) Original Auger images d) Iso-intensity lines deduced from images (a-c) for carbon (blue), sulphur (red) and aluminium (green).

For further analysis each image has been normalized to its maximum intensity and the translative offset of the different images has been corrected. By calculating iso-intensity lines of the normalized Auger image data [80% (S), 71% (C), 55% (Al)] sulphur, carbon and aluminium rich regions have been deduced. Finally the resulting data has been overlayed with the TEM image originating from the same organic nano-fiber.

References

1. Sitter, H.; Andreev, A.; Matt, G.; Sariciftci, N. S. Hot Wall Expitaxial Growth of Highly Ordered Organic Epilayers. *Synth. Met.* **2003**, *138*, 9.

2. Hernandez-Sosa, G.; Simbrunner, C.; Sitter, H. Growth and Optical Properties of α-Sexithiopene Doped Para-Sexiphenyl Nanofibers. *Appl. Phys. Lett.* **2009**, *95*, 013306.

3. Schulz, L. G. A Direct Method of Determining Preferred Orientation of a Flat Reflection Sample Using a Geiger Counter X-Ray Spectrometer. *J. Appl. Phys.* **1949**, *20*, 1030–1033.

4. Bailey, S. W. In *Structures of Layer Silicates. In Crystal Structures of Clay Minerals and Their X-ray Identification*; Brindley, G. W., Brown, G., Eds.; Mineralogical Society, London, 1980.

5. Baker, K. N.; Fratini, A. V.; Resch, T.; Knachel, H. C.; Adams, W. W.; Socci, E. P.; Farmer, B. L. Crystal Structures, Phase Transitions and Energy Calculations of poly(p-phenylene) Oligomers. *Polymer* **1993**, *34*, 1571–1587.

6. Horowitz, G.; Backet, B.; Yassar, A.; Lang, P.; Demanze, F.; Fave, J. L.; Garnier, F. Growth and Characterization of Sexithiophene Single Crystals. *Chem. Mater.* **1995**, *7*, 1337–1341.